

Research Article

Steering Parameters for Rock Grouting

Gunnar Gustafson, Johan Claesson, and Åsa Fransson

School of Civil Engineering, Chalmers University of Technology, 41296 Gothenburg, Sweden

Correspondence should be addressed to Åsa Fransson; asa.fransson@chalmers.se

Received 31 May 2013; Accepted 3 September 2013

Academic Editor: Ga Zhang

Copyright © 2013 Gunnar Gustafson et al. This is an open access article distributed under the Creative Commons Attribution License, which permits unrestricted use, distribution, and reproduction in any medium, provided the original work is properly cited.

In Swedish tunnel grouting practice normally a fan of boreholes is drilled ahead of the tunnel front where cement grout is injected in order to create a low permeability zone around the tunnel. Demands on tunnel tightness have increased substantially in Sweden, and this has led to a drastic increase of grouting costs. Based on the flow equations for a Bingham fluid, the penetration of grout as a function of grouting time is calculated. This shows that the time scale of grouting in a borehole is only determined by grouting overpressure and the rheological properties of the grout, thus parameters that the grouter can choose. Pressure, grout properties, and the fracture aperture determine the maximum penetration of the grout. The smallest fracture aperture that requires to be sealed thus also governs the effective borehole distance. Based on the identified parameters that define the grouting time-scale and grout penetration, an effective design of grouting operations can be set up. The solution for time as a function of penetration depth is obtained in a closed form for parallel and pipe flow. The new, more intricate, solution for the radial case is presented.

1. Introduction

In Swedish tunnelling pregrouting is normally used when considered necessary for the reduction of groundwater inflows. Cement grout, occasionally with plasticisers added, is preferred for economical and environmental reasons. Recently, the increased demands on tunnel tightness have led to an approach to pregrouting where the whole tunnel is systematically pregrouted according to a few predetermined standard strategies. This has led to a massive increase of performed grouting, and subsequently there is a strong need for effective design methods and steering parameters for the grouting activities.

In pregrouting a fan of boreholes is drilled around the tunnel periphery ahead of the tunnel front, grout is injected through the boreholes in order to create a low permeability zone around the tunnel, and finally the tunnel is excavated by the drill and blast method within the zone until the next cycle starts with drilling of the grouting fan. Normally grouting boreholes, 15–18 m long, are used which give 3–4 blasting rounds per cycle.

Figure 1 shows the grouting fan and some fractures as a background for the design problem. Through the borehole

grout is injected, which spreads through the fractures. At any time the grout has penetrated a distance, I , from the borehole, which is individual for each fracture. For a successful grouting the penetration between the boreholes should bridge the distance between the boreholes, L , for water-bearing fractures having a transmissivity, T , above a critical value determined by their frequency and the demands on tunnel tightness. Recent investigations of the transmissivity distributions of fractures in Swedish Precambrian crystalline rocks [1–3] have shown that only a small portion of the fractures and joints, 5–15% at a threshold level of $T = 10^{-9} \text{ m}^2/\text{s}$, are pervious and that the statistical distribution of the transmissivities of the conductive fractures is approximately lognormal.

The transmissivity is coupled to the hydraulic aperture of the fracture by the cubic law [4, 5]:

$$T = \frac{\rho_w g b^3}{12\mu_w}, \quad (1)$$

where μ_w is the viscosity, ρ_w is the density of water, and b is the so-called hydraulic aperture of the fracture. The hydraulic aperture determined by the cubic law has shown to be a good estimate for the grouting aperture [6, 7].

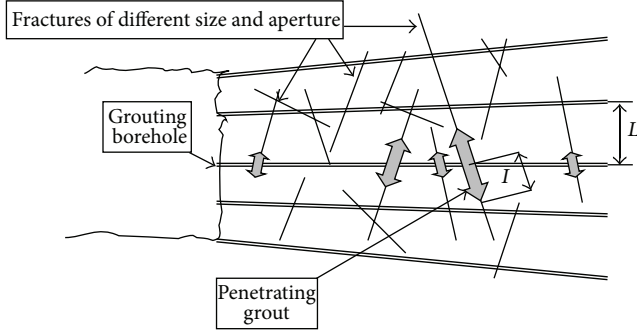


FIGURE 1: Grouting fan and grout penetration. Borehole distance L , grout penetration I .

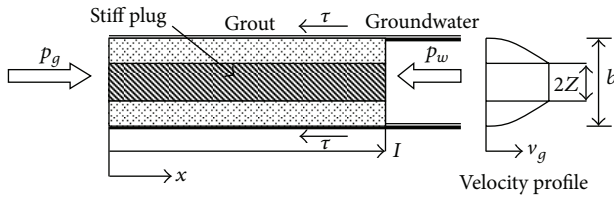


FIGURE 2: Grout penetrating a fracture.

From this it follows that in a borehole to be grouted, only a few fractures are pervious and only a small number of these contribute significantly to the groundwater flow through the rock because of the large skewness of the transmissivity distribution.

The normally used cement grouts can reasonably well be characterised as Bingham fluids [8–10]. They are thus characterised by a yield strength, τ_0 , and a plastic viscosity μ_g . From the Bingham model it follows that flow can only take place in the parts of the fluid where the internal shear stresses exceed the yield strength. This means that a stiff plug is formed in the centre of the flow channel surrounded by plastic flow zones; see Figure 2. The advance of the grout front ceases when the shear stresses at the walls of the fracture equal the yield strength of the grout. A simple force balance of the difference between the grouting and the resisting water pressures, $\Delta p = p_g - p_w$, and the shear stress gives the maximum grout penetration, I_{\max} , for a fracture of aperture b (e.g. [9, 11]):

$$I_{\max} = \frac{\Delta p \cdot b}{2\tau_0}. \quad (2)$$

The relevant design question is thus how to make sure that the penetration length is long enough to bridge the distance between the grouting boreholes for the critical fractures and the length of time it takes to reach the maximum penetration or a significant portion of it.

In order to obtain an analytical solution, the problem has to be simplified. In particular, it is assumed that the aperture is constant, not varying along the fracture. The grout properties are assumed to be constant in time. These limitations should be kept in mind when these analytical solutions are used.

2. Derivation of Equations, Results, and Discussion

2.1. *Grout Penetration.* Let $I(t)$ be the position of the grout front at time t , Figure 2. The velocity of grout, dI/dt , moving in a horizontal fracture of aperture b can according to Häßler [9] be calculated as

$$\frac{dI}{dt} = -\frac{dp}{dx} \cdot \frac{b^2}{12\mu_g} \left[1 - 3 \cdot \frac{Z}{b} + 4 \cdot \left(\frac{Z}{b} \right)^3 \right], \quad (3)$$

where

$$Z = \tau_0 \cdot \left| \frac{dp}{dx} \right|^{-1}, \quad Z < \frac{b}{2}. \quad (4)$$

Assuming parallel flow and a viscosity of the grout much higher than for water, the pressure gradient can be simplified to be

$$\frac{dp}{dx} = -\frac{\Delta p}{I}. \quad (5)$$

Equations (4), (5) and (2), give $2Z/b = I/I_{\max}$. The equation for the relative penetration depth $I_D = I/I_{\max}$ becomes from (3) after simplifications

$$\frac{dI_D}{dt} = \frac{(\tau_0)^2}{6\mu_g \Delta p} \cdot \frac{2 - 3I_D + (I_D)^3}{I_D}, \quad (6)$$

$$I_D = \frac{I}{I_{\max}} = \frac{2Z}{b}.$$

We define the characteristic time t_0 and the dimensionless time t_D :

$$t_0 = \frac{6\mu_g \Delta p}{(\tau_0)^2}, \quad t_D = \frac{t}{t_0}. \quad (7)$$

Equation (6) gives the derivative dI_D/dt_D . The derivative of t_D as a function of I_D is

$$\frac{dt_D}{dI_D} = \frac{I_D}{2 - 3I_D + (I_D)^3} = \frac{I_D}{(2 + I_D)(1 - I_D)^2}. \quad (8)$$

The right-hand function of I_D is the ratio between two polynomials, which may be expanded in partial fractions. These are readily integrated. We obtain the following explicit equation for the t_D as a function of I_D :

$$t_D = F_1(I_D), \quad F_1(s) = \frac{s}{3(1-s)} + \frac{2}{9} \cdot \ln \left[\frac{2(1-s)}{2+s} \right]. \quad (9)$$

It is straightforward to verify that derivative of (9) is given by (8) and that $I_D = 0$ for $t_D = 0$.

A plot of $I_D = I/I_{\max}$ as a function of $t_D = t/(6\mu_g \Delta p/\tau_0^2)$ is shown in Figure 3.

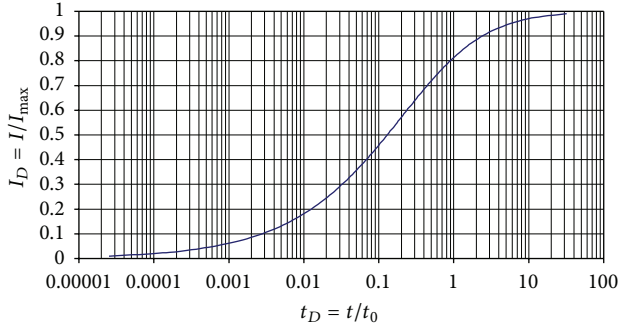


FIGURE 3: Relative penetration length as a function of dimensionless time in horizontal fracture.

From (8) and Figure 3 some interesting observations can be drawn.

- (i) The relative penetration is not a function of the fracture aperture, b . This means that the penetration process has the same time scale for all fractures with different apertures penetrated by a borehole.
- (ii) The time scale is only a function of the grouting pressure, Δp , and the grout properties, μ_g and τ_0 . Thus the parameters are decided by choice of the grouter.
- (iii) The time scale is determined by $t_0 = 6\mu_g\Delta p/\tau_0^2$ so that at this grouting time about 80% of the possible penetration length is reached in all fractures and after $5t_0$ about 95% is reached. After that the growth is very slow and the economy of continued injection could be put in doubt.

2.2. Experimental Verification. A series of grouting experiments were published by Håkansson [10]. He used thin plastic pipes instead of a parallel slot for his experiments, and several constitutive grout flow models were tested against experimental data. As could be expected more complex models could give better fit to data, but the Bingham model gave adequate results especially in the light of its simplicity.

The velocity of grout moving in a pipe of radius r_0 can be calculated to be [10]

$$\frac{dI}{dt} = -\frac{dp}{dx} \cdot \frac{(r_0)^2}{8\mu_g} \left[1 - \frac{4}{3} \cdot \frac{Z_p}{r_0} + \frac{1}{3} \cdot \left(\frac{Z_p}{r_0} \right)^4 \right], \quad (10)$$

$$Z_p = 2\tau_0 \cdot \left| \frac{dp}{dx} \right|^{-1}, \quad Z_p < r_0.$$

Here, Z_p is the radius of the plug flow in the pipe.

A force balance between the driving pressure, Δp , and the resisting shear forces inside the pipe gives the maximum grout penetration $I_{\max,p}$:

$$I_{\max,p} = \frac{\Delta p \cdot r_0}{2\tau_0}. \quad (11)$$

TABLE 1: Experimental data for grout penetration, from Håkansson [10].

Experiment	r_0 (m)	Δp (kPa)	τ_0 (Pa)	μ_g (Pa s)	$I_{\max,p}$ (m)	t_0 (s)
3 mm	0.0015	50	6.75	0.292	5.55	1922
4 mm	0.002	50	6.75	0.292	7.40	1922

Inserting (5) and (10), observing that $dx/dt = dI/dt$, and using the relative penetration depth $I_{D,p} = I/I_{\max,p}$ give after simplifications:

$$\frac{dI_{D,p}}{dt} = \frac{(\tau_0)^2}{6\mu_g\Delta p} \cdot \frac{3 - 4I_{D,p} + (I_{D,p})^4}{I_{D,p}}, \quad (12)$$

$$I_{D,p} = \frac{I}{I_{\max,p}}.$$

Inserting $t_D = t/(6\mu_g\Delta p/\tau_0^2)$, the previous equation gives the derivative $dI_{D,p}/dt_D$. The derivative of t_D as a function of $I_{D,p}$ is

$$\frac{dt_D}{dI_{D,p}} = \frac{I_{D,p}}{3 - 4I_{D,p} + (I_{D,p})^4} \quad (12')$$

$$= \frac{I_{D,p}}{[1 - I_{D,p}]^2 [3 + 2I_{D,p} + (I_{D,p})^2]}.$$

This equation may with some difficulty be integrated. We obtain the following explicit equation for the t_D as a function of $I_{D,p}$:

$$t_D = F_p(I_{D,p}),$$

$$F_p(s) = \frac{s}{6(1-s)} + \frac{1}{36} \cdot \ln \left[\frac{3(1-s)^2}{3+2s+s^2} \right] \quad (13)$$

$$- \frac{5\sqrt{2}}{36} \cdot \arctan \left(\frac{s\sqrt{2}}{s+3} \right).$$

A long, but straightforward calculation shows that the derivative satisfies (12). It is easy to see that $t_D = 0$ for $I_{D,p} = s = 0$.

In Håkansson [10] two grouting experiments in 3 and 4 mm pipes are reported. In Table 1, the relevant parameters for the experiments are shown based on the reported data. In Figure 4, a direct comparison between the function $I_{D,p}(t_D)$ and experimental data is shown.

The experimental data follow the theoretical function extremely well up to a value of $t_D \approx 2$. It shall also be borne in mind that the grout properties were taken directly from laboratory tests and no curve fitting was made. Håkansson [10], who assumed them to be a result from differences between laboratory values and experiment conditions, also identified the differences at the end of the curves. As predicted the $I_{D,p} - t_D$ -curves are almost identical for the two experiments. Another striking fact is that more than 90% of the predicted penetration is reached for $t_D \approx 2$.

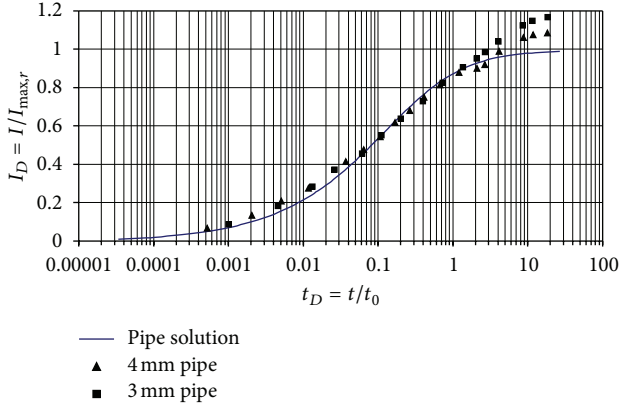


FIGURE 4: Comparison of grout penetration function in a pipe with experimental data from Håkansson [10].

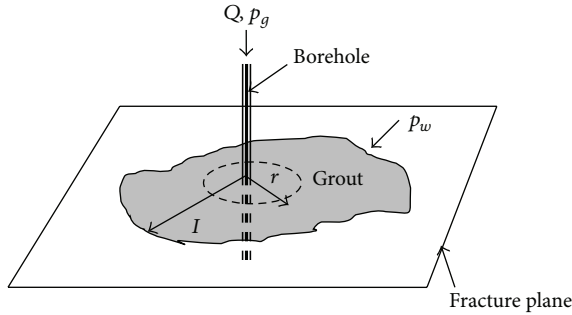


FIGURE 5: Radial penetration of grout in a fracture.

2.3. Penetration in a Two-Dimensional Fracture. A more realistic model of a fracture to grout is perhaps a pseudo-plane with a system of conductive areas and flow channels [5]. If the transmissivity of the fracture is reasonably constant, a parallel plate model with constant aperture b can approximate it. If it is grouted through a borehole, there will be a radial, two-dimensional, flow of grout out from the borehole; see Figure 5. In reality, however, the flow will as for flow of water from a borehole be something in between a system of one-dimensional channels and radial flow [12].

Equations (3) and (4) give the grout flow in the plane case. The grout flow velocity is constant (in x) and equal to the front velocity dI/dt . In the radial case we replace x by r . The grout flow velocity v_g (m/s) decreases as $1/r$, [16]. Let r_b be the radius of the injection borehole, and let $r_b + I$ be the radius of the grout injection front at any particular time t . We have

$$v_g = -\frac{dp}{dr} \cdot \frac{b^2}{12\mu_g} \left[1 - 3 \cdot \frac{Z}{b} + 4 \cdot \left(\frac{Z}{b} \right)^3 \right], \quad r_b \leq r \leq r_b + I, \quad (14)$$

where

$$Z = \tau_0 \cdot \left| \frac{dp}{dr} \right|^{-1}, \quad Z < \frac{b}{2}. \quad (15)$$

Let the grout injection rate be Q (m^3/s). The total grout flow is the same for all r :

$$Q = 2\pi r b \cdot v_g, \quad r_b \leq r \leq r_b + I. \quad (16)$$

Combing (14) and (16), we get after some calculation the following implicit differential equation for the pressure as a function of the radius:

$$\frac{6\mu_g Q}{\pi b^2 \tau_0} \cdot \frac{1}{r} = s \cdot [2 - 3 \cdot s^{-1} + s^{-3}], \quad (17)$$

$$s = \frac{b}{2Z} = \frac{b}{2\tau_0} \cdot \left| \frac{dp}{dr} \right|$$

or

$$r = \frac{2\mu_g Q}{\pi b^2 \tau_0} \cdot \frac{3s^2}{2s^3 - 3s^2 + 1}, \quad s = -\frac{b}{2\tau_0} \cdot \frac{dp}{dr}, \quad (18)$$

$$r_b \leq r \leq r_b + I.$$

The injection excess pressure is Δp . We have the boundary condition

$$p(r_b) - p(r_b + I) = \Delta p. \quad (19)$$

Here, we neglect a pressure fall in the ground water, since the viscosity of grout is much larger than that of water.

The solution $p(r)$ of (18)-(19) has the front position I as parameter. The value of Q has to be adjusted so that the pressure difference Δp is obtained in accordance with (19). The front position $I = I(t)$ increases with time. The flow velocity at the grout front $r = r_b + I(t)$ is equal to the time derivative of $I(t)$. We have from (16)

$$Q(I) = 2\pi b \cdot [r_b + I(t)] \cdot \frac{dI}{dt}, \quad I(0) = 0. \quad (20)$$

This equation determines the motion of the grout front. It depends on the required grout injection rate $Q(I)$, which is obtained from the solution of (18)-(19) for each front position I .

The solution for radial grout flow is much more complicated than for the plain case and the pipe case. We must first solve the implicit differential equation for $p(r)$. This involves the solution of a cubic equation in order to get the derivative dp/dr and an intricate integration in order to get $p(r)$. From the solution, we get the required grout flux for any front position I .

With known function $Q(I)$, we may determine the motion of the grout front from (20) by integration.

The front position I increases from zero at $t = 0$ to a maximum value for infinite time. Then the flux Q must be zero. Equation (18) gives $Q = 0$ for $s = 1$. Then we have a linear pressure variation:

$$Q = 0, \quad s = 1 \implies -\frac{dp}{dr} = \frac{2\tau_0}{b} \implies p = K - \frac{2\tau_0}{b} \cdot r. \quad (21)$$

Here, K is a constant. The boundary condition (19) determines the maximum value of I :

$$p(r_b) - p(r_b + I_{\max}) = \frac{2\tau_0}{b} \cdot (-r_b + r_b + I_{\max}) = \Delta p \implies I_{\max} = \frac{b\Delta p}{2\tau_0}. \quad (22)$$

We get the same value (2) as in the plain case.

The complete solution in the radial case involves the following constants:

$$\begin{aligned} I_{\max} &= \frac{b\Delta p}{2\tau_0}, & \gamma &= \frac{I_{\max}}{r_b} = \frac{b\Delta p}{2r_b\tau_0}, \\ t_0 &= \frac{6\mu_g\Delta p}{(\tau_0)^2}, & Q_0 &= \frac{6\pi b(I_{\max})^2}{t_0} = \frac{\pi b^3\Delta p}{4\mu_g}. \end{aligned} \quad (23)$$

2.4. Solution for the Pressure. In the dimensionless solution for the pressure, we use the borehole radius as scaling length:

$$r' = \frac{r}{r_b}, \quad I' = \frac{I}{r_b}, \quad r_b \leq r \leq r_b + I \iff 1 \leq r' \leq 1 + I'. \quad (24)$$

The pressure is scaled by $\Delta p/\gamma$. The variable s for the derivative of the pressure in (18) becomes

$$\begin{aligned} p' &= \frac{\gamma \cdot (p - p_w)}{\Delta p} \implies s = \frac{b}{2\tau_0} \cdot \left(-\frac{dp}{dr}\right) \\ &= -\frac{b\Delta p/\gamma}{2\tau_0 r_b} \cdot \frac{dp'}{dr'} = -\frac{dp'}{dr'}. \end{aligned} \quad (25)$$

The dimensionless form of (18)-(19) becomes after some recalculations

$$\begin{aligned} r' &= Q' \cdot g\left(-\frac{dp'}{dr'}\right), & g(s) &= \frac{3s^2}{2s^3 - 3s^2 + 1}, \\ Q' &= \frac{2\mu_g Q}{\pi b^2 \tau_0 r_b}, & p'(1) - p'(1 + I') &= \gamma, \\ & & 1 \leq r' &\leq 1 + I'. \end{aligned} \quad (26)$$

This is the basic equation to solve for the pressure distribution. It is to be solved for $0 < I' < \gamma$ for positive values of the parameter γ .

The solution is derived in detail in [14]. A brief derivation is presented in the appendix. The dimensionless pressure is given by

$$p'(r') = \gamma - Q' \cdot \left[\bar{G}(Q') - \bar{G}\left(\frac{Q'}{r'}\right) \right], \quad 1 \leq r' \leq 1 + I'. \quad (27)$$

The composite function $\bar{G}(q)$, which is used for $q = Q'$ and $q = Q'/r'$, is defined by

$$\begin{aligned} \bar{G}(q) &= G(\bar{s}(q)), \\ \bar{s}(q) &= \frac{1}{2\sqrt{1+q} \cdot \sin\left\{(1/3) \cdot \arcsin\left[(1+q)^{-1.5}\right]\right\}}, \\ G(s) &= \frac{4}{3} \cdot \ln(s-1) + \frac{1}{6} \cdot \ln(2s+1) - \frac{1}{s-1} \\ &\quad - \frac{3s^3}{(2s+1)(s-1)^2}. \end{aligned} \quad (28)$$

The function $\bar{s}(q)$ is the root to the cubic equation $q \cdot g(s) = 1$ for $s > 1$. The function $G(s)$ is an integral of $s \cdot dg/ds$.

The value of the factor Q' has to be chosen so that the total pressure difference corresponds to the injection pressure, (26). This gives

$$\gamma = Q' \cdot \left[\bar{G}(Q') - \bar{G}\left(\frac{Q'}{1+I'}\right) \right]. \quad (29)$$

This equation determines Q' as a function of I' and γ :

$$Q' = f'(I', \gamma), \quad 0 \leq I' \leq \gamma, \quad \gamma > 0. \quad (30)$$

The value of Q' for $I' = \gamma$ is zero in accordance with (21)-(22): $f'(\gamma, \gamma) = 0$.

2.5. Motion of Grout Front. In the dimensionless formulation of the equation for the motion of the grout front, we use I_{\max} as scaling length. We also use Q_0 and t_0 from (23)

$$\begin{aligned} I_D &= \frac{I}{I_{\max}}, & I' &= \gamma I_D, \\ Q_D &= \frac{Q}{Q_0}, & t_D &= \frac{t}{t_0}. \end{aligned} \quad (31)$$

The grout flux becomes from (23) and (26)

$$\frac{Q_0}{\gamma} = \frac{\pi b^2 \tau_0 r_b}{2\mu_g} \implies Q = \frac{Q_0}{\gamma} \cdot f'(I', \gamma) = Q_0 \cdot Q_D(I_D, \gamma). \quad (32)$$

The dimensionless grout flux is then

$$Q_D(I_D, \gamma) = \frac{f'(\gamma I_D, \gamma)}{\gamma}, \quad 0 \leq I_D \leq 1. \quad (33)$$

The dimensionless equation for the front motion is now from (32), (20), (31), and (23)

$$\begin{aligned} \frac{Q_0}{\gamma} \cdot f'(\gamma I_D, \gamma) &= 2\pi b \cdot \frac{(I_{\max})^2}{t_0} \cdot \left(\frac{1}{\gamma} + I_D\right) \cdot \frac{dI_D}{dt_D} \\ \text{or } \frac{dt_D}{dI_D} &= \frac{\gamma}{3} \cdot \frac{1/\gamma + I_D}{f'(\gamma I_D, \gamma)}. \end{aligned} \quad (34)$$

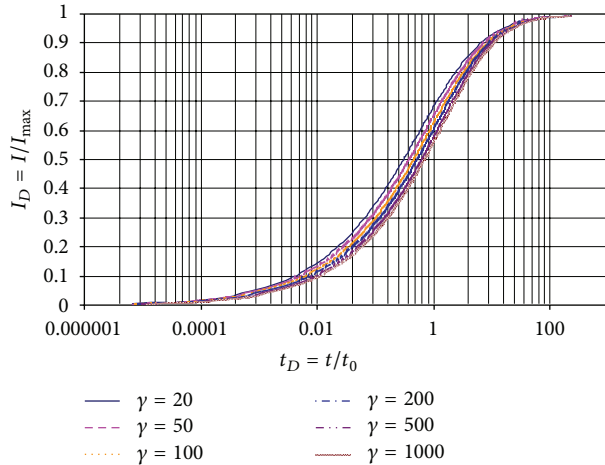


FIGURE 6: Grout penetration function $I_D = I_D(t_D, \gamma)$ for radial flow.

By integration we get the time $t_D = t/t_0$ as an integral in I_D :

$$t_D = \frac{1}{3} \cdot \int_0^{I_D} \frac{1 + \gamma I_D'}{f(\gamma I_D', \gamma)} dI_D', \quad 0 \leq I_D < 1. \quad (35)$$

We get t_D as a function of the grout front position I_D . Also in this case the inverse function describes the relative penetration as a function of the dimensionless grouting time. Figure 6 shows this relation for a few γ -values.

A comparison of Figures 3, 4, and 6 shows that the curves for $I_D(t_D)$ are similar for the three flow cases. The main difference to parallel flow is that penetration is somewhat slower for the radial case. Around 80% of maximum penetration is reached after $3t_0$ and to reach 90% takes about $7t_0$. The principle is, however, the same and the curves could be used in the same way.

2.6. Injected Volume of Grout. The injected volume of grout as a function of time is of interest. The volume is

$$\begin{aligned} V_g(t) &= \pi b \left[(r_b + I(t))^2 - (r_b)^2 \right] \\ &= \pi b I(t)^2 \cdot \left[1 + \frac{2r_b}{I(t)} \right]. \end{aligned} \quad (36)$$

Let $V_{g,\max}$ be maximum injection volume and V_D the dimensionless volume of injected grout:

$$V_D = \frac{V_g}{V_{g,\max}}, \quad V_{g,\max} = \pi b (I_{\max})^2 \cdot \left[1 + \frac{2}{\gamma} \right]. \quad (36')$$

Then we get, using (31), (24), (23), and the relation (35) between I_D and t_D ,

$$V_D(t_D, \gamma) = (I_D)^2 \cdot \frac{1 + 2/(\gamma I_D)}{1 + 2/\gamma}, \quad I_D = I_D(t_D, \gamma). \quad (37)$$

Equations presented in this paper have been used in Gustafson and Stille [15] when considering stop criteria for grouting. Grouting projects where estimates of penetration

length have been made are, for example, [13, 15, 16]. Penetration length has also been a key to presenting a concept for estimation of deformation and stiffness of fractures based on grouting data [13]. In addition to grouting of tunnels, theories have also been applied for grouting of dams [18].

3. Conclusions

The theoretical investigation of grout spread in one-dimensional conduits and radial spread in plane parallel fractures have shown very similar behavior for all the investigated cases. The penetration, I , can be described as a product of the maximum penetration, $I_{\max} = \Delta p \cdot \tau_0 / 2b$, and a time-dependent scaling factor, $I_D(t_D)$, the relative penetration length. Here Δp is the driving pressure, τ_0 is the yield strength of the grout, and b is the aperture of the penetrated fracture. The time factor or dimensionless grouting time, $t_D = t/t_0$, is the ratio between the actual grouting time, t , and a time scaling factor, $t_0 = 6\mu_g \Delta p / \tau_0^2$, the characteristic grouting time. Here μ_g is the Bingham viscosity of the grout. The relative penetration depth has a value of 70–90% for $t = t_0$ and reaches a value of more than 90% for $t > 7t_0$ for all fractures.

From this a number of important conclusions can be drawn.

- (i) The relative penetration is the same in all fractures that a grouted borehole cuts. This means that given the same grout and pressure the grouting time should be the same in high and low yielding boreholes in order to get the same degree of tightening of all fractures. This means that the tendency in practice to grout for a shorter time in tight boreholes will give poor results for sealing of fine fractures.
- (ii) The maximum penetration is governed by the fracture aperture and pressure and yield strength of the grout. The latter are at the choice of the grouter.
- (iii) The relative penetration, which governs much of the final result, is determined by the grouting time.
- (iv) The pressure and the grout properties determine the desired grouting time. These are the choice of the grouter alone.
- (v) It is poor economy to grout for a longer time than about $5t_0$ since the growth of the penetration is very slow for a time longer than that. On the other hand, if the borehole takes significant amounts of grout after $5t_0$, there is reason to stop since it indicates an unrestricted outflow of grout somewhere in the system.

The significance of this for grouting design is as follows.

- (i) The conventional stop criteria based on volume or grout flow can be replaced by a minimum time criterion based only on the parameters that the grouter can choose, that is, grouting pressure and yield strength of the grout.

- (ii) Based on an assessment of how fine fractures it is necessary to seal, a maximum effective borehole distance can be predicted given the pressure and the properties of the grout.
- (iii) The time needed for effective grouting operations can be estimated with better accuracy.
- (iv) In order to avoid unrestricted grout pumping also a maximum grouting time can be given, where further injection of grout will be unnecessary.

Appendix

Derivation of the Solution for the Pressure

We seek the solution $p'(r')$ to (26):

$$r' = Q' \cdot g \left(-\frac{dp'}{dr'} \right), \quad 1 \leq r' \leq 1 + I', \quad (\text{A.1})$$

$$g(s) = \frac{3s^2}{2s^3 - 3s^2 + 1}, \quad 0 \leq I' \leq \gamma.$$

Here, $1 + I'$ is the position of the grout front. The parameter γ is positive. Taking zero pressure at the grout front, the boundary conditions for the dimensionless pressure become

$$p'(1) = \gamma, \quad p'(1 + I') = 0. \quad (\text{A.2})$$

The dimensionless grout flux Q' is to be chosen so that the previous boundary conditions are fulfilled. The value of Q' will depend on the front position I' .

Solution in Parameter Form. In order to see more directly the character of the equation, we make the following change of notation:

$$x \longleftrightarrow r', \quad y \longleftrightarrow -p', \quad f(s) = Q' \cdot g(s). \quad (\text{A.3})$$

The equation is then of the following type:

$$x = f \left(\frac{dy}{dx} \right). \quad (\text{A.4})$$

There is a general solution in a certain parameter form to this type of implicit ordinary differential equation [19]. The solution is

$$x(s) = f(s), \quad y(s) = s \cdot f(s) - \int^s f(s') ds'. \quad (\text{A.5})$$

We have to show that this is indeed the solution. We have

$$\frac{dx}{ds} = \frac{df}{ds}, \quad \frac{dy}{ds} = 1 \cdot f(s) + s \cdot \frac{df}{ds} - f(s) = s \cdot \frac{df}{ds}. \quad (\text{A.6})$$

The ratio between these equations gives that s is equal to the derivative dy/dx . We have

$$\frac{dy}{dx} = \frac{dy/ds}{dx/ds} = s \implies f \left(\frac{dy}{dx} \right) = f(s) = x. \quad (\text{A.7})$$

The right-hand equation shows that (A.5) is the solution to (A.4).

Explicit Solution. Applying this technique to (A.1), we get the solution

$$r' = Q' \cdot g(s),$$

$$-p'(s) = s \cdot Q' \cdot g(s) - Q' \cdot \int^s g(s') ds'. \quad (\text{A.8})$$

We introduce the inverse to $g(s)$ in the following way:

$$1 = q \cdot g(s) \iff s = g^{-1} \left(\frac{1}{q} \right) = \bar{s}(q) \iff 1 = q \cdot g(\bar{s}(q)). \quad (\text{A.9})$$

The pressure with a free constant K for the pressure level may now be written as

$$p'(s) = Q' \cdot G(s) + K, \quad G(s) = \int^s g(s') ds' - s \cdot g(s). \quad (\text{A.10})$$

The solution is then from (A.8)–(A.10) (with $q = Q'/r'$)

$$p'(s) = Q' \cdot G(s) + K, \quad s = \bar{s} \left(\frac{Q'}{r'} \right) \quad (\text{A.11})$$

or, introducing the composite function $\tilde{G}(q)$,

$$\tilde{G}(q) = G(\bar{s}(q)), \quad p'(r') = Q' \cdot \tilde{G} \left(\frac{Q'}{r'} \right) + K. \quad (\text{A.12})$$

The boundary condition (A.2) at $r' = 1$ is fulfilled for a certain choice of K . The explicit solution is

$$p'(r') = \gamma - Q' \cdot \left[\tilde{G}(Q') - \tilde{G} \left(\frac{Q'}{r'} \right) \right], \quad 1 \leq r' \leq 1 + I'. \quad (\text{A.13})$$

The other boundary condition (A.2) at $r' = 1 + I'$ is fulfilled when Q' satisfies the equation

$$\gamma = Q' \cdot \left[\tilde{G}(Q') - \tilde{G} \left(\frac{Q'}{1 + I'} \right) \right]. \quad (\text{A.14})$$

We note that the derivative $-dp'/dr'$ is given by s :

$$s = -\frac{dp'}{dr'}. \quad (\text{A.15})$$

The pressure derivative is equal to -1 for zero flux, (21) and (25), in the final stagnant position $I' = \gamma$. The magnitude of this derivative is larger than 1 for all preceding positions $I' < \gamma$. This means that s is larger than (or equal to) 1 in the solution.

The Function $G(s)$. The solution (A.13) and the composite function (A.12) involve the function $G(s)$ defined in (A.10)

and (A.1). The integral of $g(s)$ is obtained from an expansion in partial fractions. We have

$$\begin{aligned} g(s) &= \frac{3s^2}{2s^3 - 3s^2 + 1} = \frac{3s^2}{(2s+1)(s-1)^2} \\ &= \frac{1}{3} \cdot \frac{1}{2s+1} + \frac{4}{3} \cdot \frac{1}{s-1} + \frac{1}{(s-1)^2}. \end{aligned} \quad (\text{A.16})$$

The integral of $g(s)$ is readily determined. The function $G(s)$ becomes from (A.10) and (A.16)

$$\begin{aligned} G(s) &= \frac{1}{6} \cdot \ln(2s+1) + \frac{4}{3} \cdot \ln(s-1) - \frac{1}{s-1} \\ &\quad - \frac{3s^3}{2s^3 - 3s^2 + 1}, \quad s > 1. \end{aligned} \quad (\text{A.17})$$

We will use the function for $1 < s < \infty$.

The Inverse $\bar{s}(q)$. The inverse (A.9) is, for any $q \geq 0$, the solution of the cubic equation

$$2s^3 - 3s^2 + 1 = 3qs^2. \quad (\text{A.18})$$

The solution is reported in detail in [14]. The cubic equation has three real-valued solutions for positive q -values, one of which is larger than 1 (for $q = 0$ there is a double root $s = 1$ and a third root $s = -0.5$, (A.16)). We need the solution $s > 1$. It is given by

$$\bar{s}(q) = \frac{1}{2\sqrt{1+q} \cdot \sin\left\{\frac{1}{3} \cdot \arcsin\left[(1+q)^{-1.5}\right]\right\}}, \quad q \geq 0. \quad (\text{A.19})$$

A plot shows that $\bar{s}(q)$ is an increasing function from $\bar{s}(0) = 1$ for $q \geq 0$. It has the asymptote $1.5 \cdot (1+q)$ for large q .

We will show that (A.19) is the inverse. We use the notations

$$\begin{aligned} \bar{s}(q) = s &= \frac{1}{2\sqrt{1+q} \cdot \sin(\phi/3)}, \\ \phi &= \arcsin\left[(1+q)^{-1.5}\right]. \end{aligned} \quad (\text{A.20})$$

In (A.18), we put $3qs^2$ on the left-hand side, divide by s^3 , and insert $s = \bar{s}(q)$ from (A.20). Then we have

$$\begin{aligned} &\left(\frac{1}{s}\right)^3 - 3(1+q) \cdot \frac{1}{s} + 2 \\ &= \left(2\sqrt{1+q} \cdot \sin\left(\frac{\phi}{3}\right)\right)^3 - 3(1+q) \cdot 2\sqrt{1+q} \cdot \sin\left(\frac{\phi}{3}\right) + 2 \\ &= 2 - 2 \cdot (1+q)^{1.5} \cdot \left[3 \cdot \sin\left(\frac{\phi}{3}\right) - 4 \cdot \sin^3\left(\frac{\phi}{3}\right)\right] \\ &= 2 - 2 \cdot (1+q)^{1.5} \cdot \sin(\phi) \\ &= 2 - 2 \cdot (1+q)^{1.5} \cdot (1+q)^{-1.5} \\ &= 0. \end{aligned} \quad (\text{A.21})$$

On the third line we use a well-known trigonometric formula relating $\sin(\phi/3)$ to $\sin(\phi)$. We have shown that (A.19) is the inverse.

Symbols and Units

b (m):	Fracture aperture
I (m):	Penetration length of injected grout
I_{\max} (m):	Maximum penetration length of grout
$I_{\max,p}$ (m):	Maximum penetration length of grout in a pipe
I' (—):	Ratio between penetration and borehole radius
I_D (—):	Relative penetration length
$I_{D,p}$ (—):	Relative penetration length in a pipe
L (m):	Distance between grouting boreholes
p (Pa):	Pressure
p_D (—):	Dimensionless pressure
p_g (Pa):	Grout pressure
p_w (Pa):	Water pressure
Q (m ³ /s):	Grout injection flow rate
r (m):	Pipe radius, radial distance from borehole centre
r_b (m):	Borehole radius
r_D (—):	Dimensionless radius
r_p (m):	Grout plug radius
r_0 (m):	Pipe radius
r' (—):	Ratio between distance from borehole centre and borehole radius
T (m ² /s):	Transmissivity
t (s):	Grouting time
t_0 (s):	Characteristic grouting time
t_D (—):	Dimensionless grouting time
V_g (m ³):	Injected volume of grout
V_{\max} (m ³):	Maximum grout volume in a fracture
V_D (—):	Dimensionless grout volume
x (m):	Length coordinate
Z (—):	Bingham half-plug thickness
γ (—):	Ratio between maximum penetration and borehole radius
Δp (Pa):	Driving pressure for grout
μ_g (Pas):	Plastic viscosity of grout
μ_w (Pas):	Viscosity of water
ρ_w (kg/m ³):	Density of water
τ_0 (Pa):	Yield strength of grout.

Acknowledgments

The authors would like to acknowledge the effort of Gunnar Gustafson who deceased during the study.

References

- [1] J. D. Osnes, A. Winberg, and J. E. Andersson, "Analysis of well test data—application of probabilistic models to infer hydraulic properties of fractures," Topical Report RSI-0338, RE/SPEC, Rapid City, Dakota, 1988.

- [2] C. L. Axelsson, E. K. Jonsson, J. Geier, and W. Dershowitz, "Discrete fracture modelling," SKB Progress Report 25-89-21, SKB, Stockholm, Sweden, 1990.
- [3] Å. Fransson, "Nonparametric method for transmissivity distributions along boreholes," *Ground Water*, vol. 40, no. 2, pp. 201–204, 2002.
- [4] D. T. Snow, "The frequency and apertures of fractures in rock," *International Journal of Rock Mechanics and Mining Sciences and Geomechanics Abstracts*, vol. 7, no. 1, pp. 23–40, 1970.
- [5] R. W. Zimmerman and G. S. Bodvarsson, "Hydraulic conductivity of rock fractures," *Transport in Porous Media*, vol. 23, no. 1, pp. 1–30, 1996.
- [6] Å. Fransson, "Characterisation of a fractured rock mass for a grouting field test," *Tunnelling and Underground Space Technology*, vol. 16, no. 4, pp. 331–339, 2001.
- [7] M. Eriksson, "Grouting field experiment at the Äspö Hard Rock Laboratory," *Tunnelling and Underground Space Technology*, vol. 17, no. 3, pp. 287–293, 2002.
- [8] M. Wallner, *Propagation of Sedimentation Stable Cement Pastes in Jointed Rock*, University of Aachen, Rock Mechanics and Waterways Construction, BRD, 1976.
- [9] L. Hässler, *Grouting of rock—simulation and classification [thesis]*, Department of Soil and Rock Mechanics, KTH, Stockholm, Sweden, 1991.
- [10] U. Håkansson, *Rheology of fresh cement-based grouts [thesis]*, Department of Soil and Rock Mechanics, KTH, Stockholm, Sweden, 1993.
- [11] G. Gustafson and H. Stille, "Prediction of groutability from grout properties and hydrogeological data," *Tunnelling and Underground Space Technology*, vol. 11, no. 3, pp. 325–332, 1996.
- [12] J. A. Barker, "A generalized radial flow model for hydraulic tests in fractured rock," *Water Resources Research*, vol. 24, no. 10, pp. 1796–1804, 1988.
- [13] Å. Fransson, C.-F. Tsang, J. Rutqvist, and G. Gustafson, "Estimation of deformation and stiffness of fractures close to tunnels using data from single-hole hydraulic testing and grouting," *International Journal of Rock Mechanics and Mining Sciences*, vol. 47, no. 6, pp. 887–893, 2010.
- [14] J. Claesson, "Radial bingham flow. background report of a detailed solution," Tech. Rep., Department of Building Technology, Chalmers University of Technology, Göteborg, Sweden, 2003.
- [15] G. Gustafson and H. Stille, "Stop criteria for cement grouting," *Felsbau*, vol. 23, no. 3, pp. 62–68, 2005.
- [16] L. Hernqvist, Å. Fransson, G. Gustafson, A. Emmelin, M. Eriksson, and H. Stille, "Analyses of the grouting results for a section of the APSE tunnel at Äspö Hard Rock Laboratory," *International Journal of Rock Mechanics and Mining Sciences*, vol. 46, no. 3, pp. 439–449, 2009.
- [17] C. Butrón, G. Gustafson, Å. Fransson, and J. Funehag, "Drip sealing of tunnels in hard rock: a new concept for the design and evaluation of permeation grouting," *Tunnelling and Underground Space Technology*, vol. 25, no. 2, pp. 114–121, 2010.
- [18] H. Stille, G. Gustafson, and L. Hässler, "Application of new theories and technology for grouting of dams and foundations on rock," *Geotechnical and Geological Engineering*, vol. 30, no. 3, pp. 603–624, 2012.
- [19] E. Kamke, *Differentialgleichungen. Lösungsmethoden und Lösungen*, Becker & Erler, Leipzig, Germany, 1943.